Random Response of Beams and Plates with Slipping at Support Boundaries

D. M. Tang* and E. H. Dowell†
Duke University, Durham, North Carolina

A numerical and experimental study is made of the response to random excitation of a beam and rectangular plate with dry friction damping due to slipping at the support boundaries. The design of the beam experimental apparatus and the utilization of the associated instrumentation are described. Comparisons of the experimental results with those obtained from an approximate analytical solution and from numerical simulations are made. The good agreement among these several results shows that the concept of an equivalent linear viscous damping due to slipping at the support boundaries can often be usefully applied to determine the response due to random excitation. This approach, when applicable, greatly simplifies the nonlinear random vibration problem.

Nomenclature

a	= beam or plate length, cm
a_n	= modal generalized coordinate, cm
b	= plate width, cm
C_n	= see Eq. (9)
C_{1eq}, C_{2eq}	= equivalent linear damping, 1/s
D	= plate stiffness, kg·cm
df	= bandwidth of narrow band excitation, Hz
E	= modulus of elasticity, kg/cm^2
$\langle F^2 \rangle$	= mean square input force, kg^2
$F(t)$	= force, kg
F_0	= center frequency of narrow-band excitation, Hz
f_n, ω_n	= nth mode natural frequencies of beam or plate, Hz, 1/s
h	= plate thickness, cm
I	= beam moment of inertia, cm^4
j	= $\sqrt{-1}$
K_{1eq}, K_{2eq}	= equivalent linear stiffness, 1/s^2
L	= beam length
N_g	= normal load, kg
N_x, N_y, N_{xy}	= stress resultants, kg/cm
n, n_x, n_y	= mode numbers
P_x, P_y	= stress resultants at plate edge, kg/cm
PSD	= power spectral density
S_0	= PSD of white noise excitation, kg^2/Hz
t	= time, s
w	= lateral beam or plate displacement, cm
$\langle w^2 \rangle$	= mean square response, cm^2
x, y	= Cartesian position coordinates on beam or plate
Z_1, Z_2	= see Eq. (11)
δ	= delta function
ζ_{en}	= see Eq. (18)
ζ_n	= modal critical damping ratio
λ	= see Eq. (19), cm^2/kg^2
μ	= coefficient of friction
μ_p	= Poisson's ratio
ϕ_n	= modal function
$(\dot{})$	= time derivative

Received Sept. 20, 1985; revision received Jan. 3, 1986.

*Visiting Scholar (from Nanjing Aeronautical Institute, China), Department of Mechanical Engineering and Materials Science.
†Dean, School of Engineering.

Introduction

In Ref. 1 and its companion paper,[2] an approximate analytical solution for a pinned beam and pinned plate with dry friction due to slipping at the support boundaries was derived. Numerical and experimental studies were described and sinusoidal excitation considered. The purpose of this paper is to consider the response to random noise excitation.

The equivalent linear viscous damping concept proposed in Ref. 1 can still be applied as an approximation. A comparison between an approximate solution obtained using this concept and numerical simulation is also made. The generally good agreement shows that the equivalent linear viscous damping, which was originally derived for sinusoidal excitation, often also can be usefully applied to random excitation. This approach greatly simplifies the nonlinear random vibration problem.

For the random response of a pinned plate model, two kinds of nonlinear characteristics are involved in the system: damping and stiffness nonlinearities. For large-amplitude motion or light damping, the stiffness nonlinearity in the system is often very important. The statistical linearization technique is applied to analyze this system. This method is based on the well-known work on equivalent linearization of Kryloff and Bogoliubov. The extension of this technique to problems of random excitation was made by Booton[3] and Caughey,[4] and a further extension of Caughey's normal model approach was made by Atalik[5] and Fang and Wang.[6] Using this method, we obtain good results for the case of small equivalent damping and large amplitude. We also discuss random response for the case of stick or slip-stick motion at the edges for both the beam and plate based upon numerical simulations. These results will be of interest for understanding the effect of dry fiction at the support edges on the response amplitude.

The design of the beam experimental apparatus and the utilization of the associated instrumentation are also described in this paper. Comparisons of the experimental results to those obtained from the approximate solution and numerical time integration are carried out to confirm the range of accuracy of the analytical approach. In general, the experimental results are reasonably close to those of the theoretical solutions. But there are some quantitative differences, which come mainly from differences in the measured and theoretically assumed input random forces. These are explained in the text.

Theoretical Analysis: Approximate Solution

Pinned-Pinned Beam

The lateral equation of motion of a beam is well known,

$$EI\frac{\partial^4 w}{\partial x^4}-N_x\frac{\partial^2 w}{\partial x^2}+m\frac{\partial^2 w}{\partial t^2}=F(t)\delta(x-x_F) \tag{1}$$

where, $F(t)$ is the random exciting force and an assumption of white noise excitation is made in order to simplify the problem. The exciting force is concentrated at point $x=x_F$, as shown in Fig. 1. N_x is the in-plane stress resultant due to in-plane dry friction sliding action.

A Galerkin type modal solution method will be used. Thus, w is represented as

$$w=\sum_n a_n(t)\phi_n(x) \tag{2}$$

where, for a uniform simply supported beam, the natural vibration modes are

$$\phi_n(x)=\sin(n\pi x/a)$$

Reference 1 proposed a formula for an equivalent modal viscous damping due to dry friction when slip occurs,

$$\zeta_n=\frac{\mu Ng}{\pi\omega_n}\frac{1}{\sqrt{EIm^*}} \tag{3}$$

It is found from Eqs. (1-3) that (also see Refs. 1 and 2)

$$(am/2)(\ddot{a}_n+2\zeta_n\omega_n\dot{a}_n+\omega_n^2 a_n)=F(t)\phi_n(x_F) \tag{4}$$

From Eq. (4), the frequency response function $H_n(\omega)$ is

$$H_n(\omega)=\frac{1}{(am/2)(\omega_n^2-\omega^2+2j\zeta_n\omega\omega_n)} \tag{5}$$

The mean square response of $w(x,t)$ follows as[7]

$$\langle w^2\rangle=\sum_n\phi_n^2(x)\phi_n^2(x_F)S_0\int_0^\infty H_n(\omega)H_n^*(\omega)\mathrm{d}\omega \tag{6}$$

where $H_n^*(\omega)$ is the complex conjugate of $H_n(\omega)$.

For well-separated (in frequency) modes, the mean square response can be approximately written using Eqs. (3) and (6) as

$$\langle w^2\rangle=U_b/Ng \tag{7}$$

where

$$U_b=\frac{2S_0}{\mu m}\sum_n\phi_n^2(x)\phi_n^2(x_F)\frac{1}{n^2\omega_n}$$

Pinned Rectangular Plate

A More Accurate, Approximate Solution

The lateral equation of motion of a rectangular plate is

$$D\nabla^4 w-N_x\frac{\partial^2 w}{\partial x^2}-N_y\frac{\partial^2 w}{\partial y^2}-2N_{xy}\frac{\partial^2 w}{\partial x\partial y}$$

$$+m\frac{\partial^2 w}{\partial t^2}=F(t)\delta(x-x_F)\delta(y-y_F) \tag{8}$$

where, $F(t)$ is the white noise excitation force, concentrated at point $x=x_F$, $y=y_F$, as shown in Fig. 2.

We assume that the solution of Eq. (8) has the form

$$w\left(a_1\sin\frac{\pi x}{a}+a_2\sin\frac{2\pi x}{a}\right)\sin\frac{\pi y}{b}$$

We are in the fortunate position of being able to make use of much of the analysis done by Fralich.[8] See Refs. 1 and 2 for the details of the analysis. The final nondimensional equations are represented as

$$C_1''+(-M_1+P_1C_1^2+QC_2^2)C_1=\bar{F}_1$$

$$C_2''+(-M_2+P_2C_2^2+QC_1^2)C_2=\bar{F}_2 \tag{9}$$

where

$$M_1=\bar{P}_x+\nu^2\bar{P}_y-(1+\nu^2)^2$$

$$M_2=4\bar{P}_x+\nu^2\bar{P}_y-(4+\nu^2)^2$$

$$\bar{P}_x=P_xa^2/\pi^2D,\quad \bar{P}_y=P_ya^2/\pi^2D,\quad C_n=a_n\sqrt{Eh/D}$$

$$P_1=\frac{1}{16}(1+\nu^4),\quad P_2=\frac{1}{16}(16+\nu^4),\quad \nu=\frac{a}{bn_y}$$

$$Q=\frac{1}{4}(1+\nu^4)+\frac{81\nu^4}{16(1+4\nu^2)^2}+\frac{\nu^4}{16(9+4\nu^2)^2}$$

$$\bar{F}_1=\frac{4a^4}{\pi^4Dab}\sqrt{\frac{Eh}{D}}F(t)\sin\frac{\pi}{a}x_F\cdot\sin\frac{\pi}{b}y_F$$

$$\bar{F}_2=\frac{4a^4}{\pi^4Dab}\sqrt{\frac{Eh}{D}}F(t)\sin\frac{2\pi}{a}x_F\cdot\sin\frac{\pi}{b}y_F$$

and where $(\,)'$ denotes differentiation with respect to τ,

$$\tau=\frac{\pi^2}{a^2}\sqrt{\frac{D}{m}}t$$

When slipping occurs at both plate edges, $x=a$ and $y=b$, we introduce an equivalent linear viscous critical damping

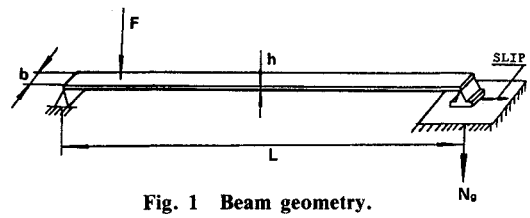

Fig. 1 Beam geometry.

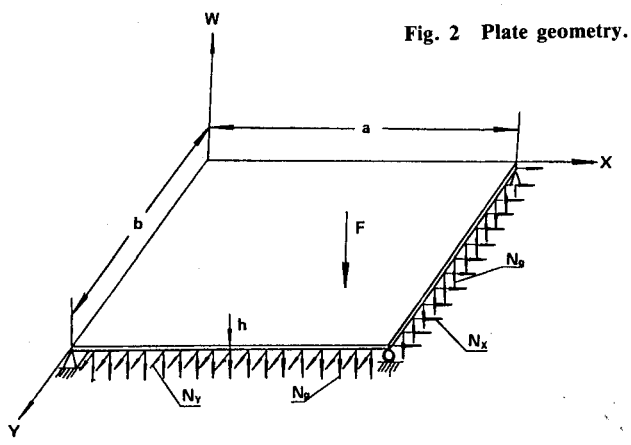

Fig. 2 Plate geometry.

ratio that is derived in Ref. 1. as

$$\zeta_n = \frac{\mu N_g}{\pi} \frac{1}{\omega_n \sqrt{Dm}} \tag{10}$$

In this case, Eq. (9) will be approximately replaced by a set of new equivalent equations having an equivalent linear damping and nonlinear stiffness terms. One finds that

$$\ddot{Z}_1 + 2\zeta_1\omega_1\dot{Z}_1 + \omega_1^2 Z_1 + P_{Z_1} Z_1^3 + Q_Z Z_1 Z_2^2 = f_1(t)$$
$$\ddot{Z}_2 + 2\zeta_2\omega_z\dot{Z}_2 + \omega_2^2 Z_2 + P_{Z_2} Z_2^3 + Q_Z Z_1^2 Z_2 = f_2(t) \tag{11}$$

where

$$P_{Z_1} = \frac{\pi^4 D}{a^4 m} P_1, \quad P_{Z_2} = \frac{\pi^4 D}{a^4 m} P_2$$

$$f_1(t) = G_1 F(t), \quad f_2(t) = G_2 F(t)$$

$$G_1 = \frac{4}{abm}\sqrt{\frac{Eh}{D}} \sin\frac{\pi}{a}x_F \sin\frac{\pi}{b}y_F$$

$$G_2 = \frac{4}{abm}\sqrt{\frac{Eh}{D}} \sin\frac{2\pi}{a}x_F \sin\frac{\pi}{b}y_F$$

$$Q_Z = \frac{\pi^4 D}{a^4 m} Q, \quad Z_1 = a_1\sqrt{\frac{Eh}{D}}, \quad Z_2 = a_2\sqrt{\frac{Eh}{D}}$$

To solve Eq. (11) the statistical linearization technique can be directly applied. Equation (11) can be rewritten as an equivalent set of completely linear equations in the following form:

$$\ddot{Z}_1 + C_{1eq}\dot{Z}_1 + K_{1eq} Z_1 = f_1(t)$$
$$\ddot{Z}_2 + C_{2eq}\dot{Z}_2 + K_{2eq} Z_2 = f_2(t) \tag{12}$$

According to Caughey's equivalent linearization technique with random excitation,[4,6] these coefficients are represented as

$$C_{1eq} = 2\zeta_1\omega_1 + 2Q_Z\langle Z_1 Z_2\rangle\langle \dot{Z}_1 Z_2\rangle / \langle \dot{Z}_1^2\rangle$$
$$C_{2eq} = 2\zeta_2\omega_2 + 2Q_Z\langle Z_1 Z_2\rangle\langle Z_1 \dot{Z}_2\rangle / \langle \dot{Z}_2^2\rangle$$
$$K_{1eq} = \omega_1^2 + 3P_{Z_1}\langle Z_1^2\rangle + Q_Z\langle Z_2^2\rangle + 2Q_Z\langle Z_1 Z_2\rangle^2 / \langle Z_1^2\rangle$$
$$K_{2eq} = \omega_2^2 + 3P_{Z_2}\langle Z_2^2\rangle + Q_Z\langle Z_1^2\rangle + 2Q_Z\langle Z_1 Z_2\rangle^2 / \langle Z_2^2\rangle \tag{13}$$

where $\langle Z_1^2\rangle$, $\langle Z_2^2\rangle$... are mean square values of random variables Z_1 and Z_2 and $\langle Z_2 Z_2\rangle$, $\langle Z_1 \dot{Z}_2\rangle$... the covariances of Z_1, Z_2, $\dot{Z}_1$, and $\dot{Z}_2$.

It is very evident that these coefficients depend upon random response variables. Thus, in order to find these coefficients, an iteration procedure is required. The damping and stiffness coefficients of the linear system are assigned as the initial guesses used for the solution of Eq. (12). The iteration stops when the following condition is satisfied:

$$|(C_{ieq})_{s+1} - (C_{ieq})_s| \le e$$
$$|(K_{ieq})_{s+1} - (K_{ieq})_s| \le e \tag{14}$$

where s is the number of iterations and e a given iteration error value.

Once these coefficients are obtained, the correlation function matrices of the system response are given by the formulas in Ref. 6.

Finally, the approximate solution of Eq. (8) for the mean square value $\langle w^2\rangle$ is given by

$$\langle w^2\rangle = \left(\sin^2\frac{\pi x}{a}\sin^2\frac{\pi y}{a}\langle Z_1^2\rangle + \sin^2\frac{2\pi x}{a}\sin^2\frac{\pi y}{b}\langle Z_2^2\rangle + 2\sin\frac{\pi x}{a}\sin\frac{2\pi x}{a}\sin^2\frac{\pi y}{b}\langle Z_1 Z_2\rangle\right) D \Big/ Eh \tag{15}$$

In Eq. (15), the cross term $\langle Z_1 Z_2\rangle$ is not equal to zero because Z_1 and Z_2 are correlated in Eq. (11).

A Simple, Approximate Solution

For simplicity the nonlinear stiffness term is neglected for the rectangular pinned plate and the normal force N_g is assumed to be the same on both edges of sliding contact $x=a$ and $y=b$. For a sharp resonance or low-damping system, we may obtain the mean square response formula (see Ref. 7)

$$\langle w^2\rangle = \frac{\pi}{4}\sum_n \frac{\phi_n^2(x,y)\phi_n^2(x_F,y_F)}{M_n^2\omega_n^3\zeta_n} S_0 \tag{16}$$

where $M_n = abm/4$.

Recalling Eq. (10), we may obtain

$$\langle w^2\rangle = U_p/Ng \tag{17}$$

where

$$U_p = \frac{4S_0}{\mu m b^2}\sum_n \phi_n^2(x,y)\phi_n^2(x_F,y_F)\frac{1}{\omega_n[n_x^2 + (a/b)^2 n_y^2]}$$

Theoretical Analysis: Numerical Simulation

Response to Broadband Random Excitation

Pinned-Pinned Beam

The basic equation used in numerical integration[1,2] is

$$\frac{am}{2}\left[\omega_n^2 a_n + N_x\left(\frac{n\pi}{a}\right)^2\frac{a_n}{m} + 2\zeta_{en}\omega_n\dot{a}_n + \ddot{a}_n\right] = G^* F(t)\phi_n(x_F) \tag{18}$$

where G is a variable value used to control the magnitude of random exciting force and $F(t)$ the set of standard Gaussian random numbers whose mean value is equal to zero and whose standard deviation is unity. We use a standard IMSL subroutine GGNML to generate those numbers. ζ_{en} is an equivalent viscous damping ratio of the beam material itself. For the first mode, it was found to be approximately $\zeta_{e1} = 0.006$, from a transient decay test of the experimental specimen to be discussed later. Further, as shown in Refs. 1 and 2, the in-plane stress resultant is given by

$$\text{No slip:} \quad N_x \frac{Eh}{2a}\sum_n a_n^2\left(\frac{n\pi}{a}\right)^2\frac{a}{2}$$

$$\text{Slip:} \quad N_x = \mu N g \,\text{Sign}\left[\sum_n a_n\dot{a}_n\left(\frac{n\pi}{a}\right)^2\frac{a}{2}\right]$$

The results of the numerical integration are the discrete distributions of the random time response. The mean square response $\langle w^2\rangle$ and input force $\langle F^2\rangle$ can be calculated numerically from

$$\langle w^2\rangle = \sum_{j=1}\sum_n [a_n(t_j)\phi_n^2(x)]^2/L, \quad n = 1,2,3$$

$$\langle F^2\rangle = \sum_{j=1}[G^* F(t_j)]^2/L, \quad j = 1,2,\ldots, 1024$$

Here, we introduce a ratio equal to mean square response over mean square input force, i.e.,

$$\lambda = \langle w^2 \rangle / \langle F^2 \rangle \tag{19}$$

This ratio will be used to discuss the theoretical and experimental results.

The power spectral density (PSD) of response can be obtained by using a Fourier transform of $w(t)$. In order to improve the degree of confidence, we use ensemble averaging for K times ($K > 100$); i.e., we take K samples from a very long Gaussian random signal (random numbers), calculate the mean square response from every sample, and then construct an ensemble average. The same method is followed for the response PSD.

Rectangular Plate

Equations (9) are used in the numerical time integration. Also see Refs. 1 and 2. When no slip occurs at the edges of the plate, the in-plate forces $\bar{P}_x$ and $\bar{P}_y$ at the plate edges are represented as

$$\bar{P}_x = -\frac{1}{8(1-\mu_p^2)}[C_1^2(1+\nu^2\mu_p) + C_2^2(4+\mu_p\nu^2)]$$

$$\bar{P}_y = -\frac{1}{8(1-\mu_p^2)}[C_1^2(\mu_p+\nu^2) + C_2^2(4\mu_p+\nu^2)]$$

When slip occurs, then

$$\bar{P}_x = \mu \bar{N}_g \text{Sign}(C_1 C_1' + 4C_2 C_2')$$

$$\bar{P}_y = \mu \bar{N}_g \text{Sign}(C_1 C_1' + C_2 C_2')$$

$$w = \sqrt{\frac{D}{Eh}}\left(C_1 \sin\frac{\pi x}{a} + C_2 \sin\frac{2\pi x}{a}\right)\sin\frac{\pi y}{b}$$

The ensemble averaging concept is also used in the plate calculation.

Response to Narrow-Band Random Excitation

For comparison with the results under sinusoidal excitation, the response to narrow-band random excitation is also determined. The basic equations for both the beam and plate are the same as before. The difference is in how we generate a narrow-band excitation function. A narrow-band filter is put after a white-noise source. The filter is an equivalent mechanical vibration system with a single degree of freedom. Its center frequency f_0 and bandwidth df can be adjusted.

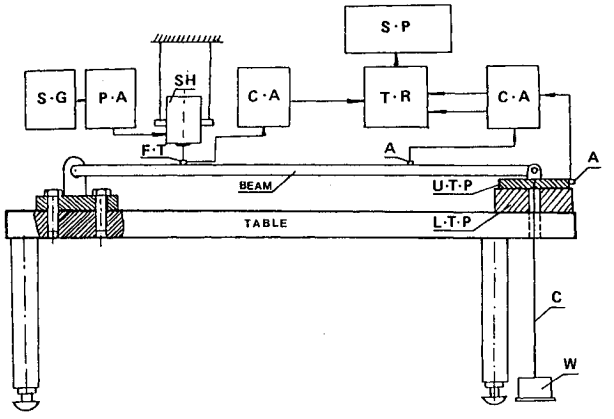

Fig. 3 Experimental setup: S.G = random signal generator, P.A = power amplifier, C.A = charge amplifier, T.R = tape recorder, S.P = signal processor Zonic 6088, SH = shaker, A = accelerometer, F.T = force transducer, U.T.P = upper test piece, L.T.P = lower test piece, W = weight, C = cable.

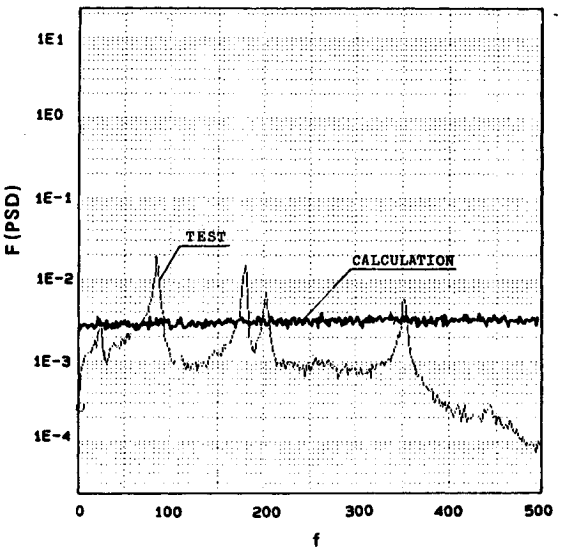

Fig. 4 Input force PSD used in the calculation and as obtained from experiment.

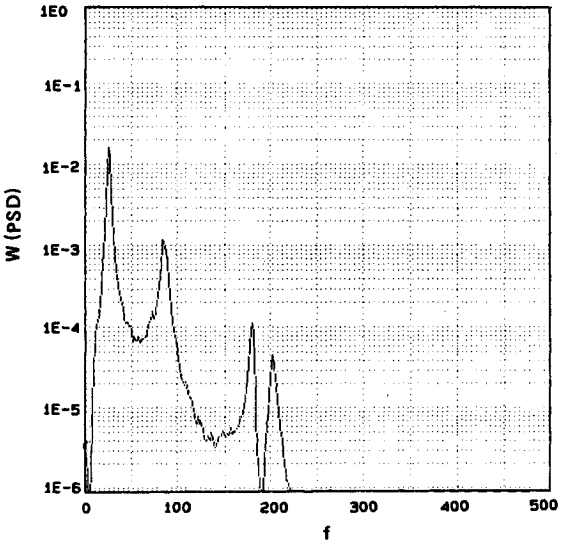

Fig. 5a Experimental response PSD for $N_g = 6$ kg.

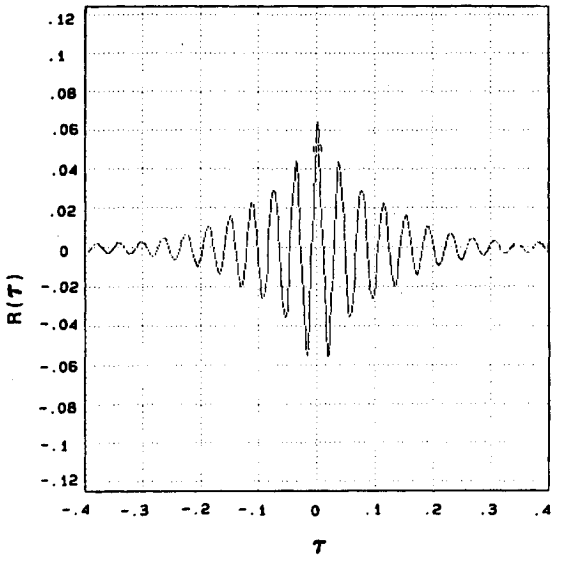

Fig. 5b Experimental response autocorrelation function for $N_g = 6$ kg.

When a broadband signal passes through the narrow-band filter, a narrow-band excitation signal (random numbers) is generated. Figure 11 shows the PSD of a narrow-band random force used in this calculation.

Numerical Examples

The approximate solution and numerical simulation of the full nonlinear equations were calculated for both a pinned beam and a rectangular pinned plate model. The purpose was to evaluate the approximate solution and to check the degree of slipping motion at the support boundaries under broadband and narrow random excitation. The parameters of the two models are listed in Table 1.

Experiment

In order to check the validity of the theoretical results, vibration tests were performed on a aluminum pinned-pinned beam. The geometric dimensions and the material properties of the model are as given before. The one pinned end is clamped on a very heavy steel table. The other pinned end has a very light aluminum upper test piece. The lower test piece is made of steel and has a polished rubbing surface that is clamped on the same table. The dry friction force is generated by the relative motion between the two test pieces held together with a constant normal load. The normal load is provided by a mass block that is hung on the center of upper test piece by a long cable. A block diagram of the experimental apparatus is shown in Fig. 3.

There are four major components of the vibration test: excitation, measurement, recording, and analysis. An electric magnetic shaker was used to excite the beam. It was driven by a random generator (B&K 1024), which provides both white and narrow-band noise. The frequency bandwidth can be chosen in three steps, 10, 30, and 100 Hz. The center frequency of the narrow-band noise can be tuned continuously. In order to reduce the effect of the additional mass of the joint components between the shaker and the beam on the beam vibration characteristics, the position of the driving point is located near the completely pinned end.

The force transducer (B&K 8200) and accelerometers (B&K 4375, 4332) are used to measure the force and acceleration responses of the beam and slip at the support boundary, respectively. The 4375 accelerometer is very lightweight (2.6 g) and is highly voltage sensitive. The charge amplifier (B&K 2635) is a portable conditioning amplifier containing intergration networks to provide a signal proportional to vibration displacement, velocity, and acceleration.

Table 1 Model parameters

Parameter	Pinned beam	Pinned plate
μ	0.158	0.158
μ_p	—	0.3
N_g	As indicated	As indicated
E, kg/cm^2	2.1×10^6	0.7×10^6
a, cm	70.3	76.2
b, cm	2.54	50.8
h, cm	0.632	0.0794
m, kg·s^2/cm^2	1.276×10^{-5}	2.17×10^{-7}
D, kg·cm	—	32.0875
ν	—	1.5
x/a	0.2561[a]	—
x_F/a	0.9075[b]	0.25
y_F/b	—	0.25
f_1, Hz	29.8	10.67 (for $n_x=1$, $n_y=1$)
f_2, Hz	119.2	20.52 (for $n_x=2$, $n_y=1$)
f_3, Hz	268.2	—
$\phi_1(x)$	0.723	—
$\phi_2(x)$	0.991	—
$\phi_3(x)$	0.631	—
$\phi_1(x_F)$	0.286	—
$\phi_2(x_F)$	0.549	—
$\phi_3(x_F)$	0.621	—

[a]Location of measurement point. [b] Location of driving force point.

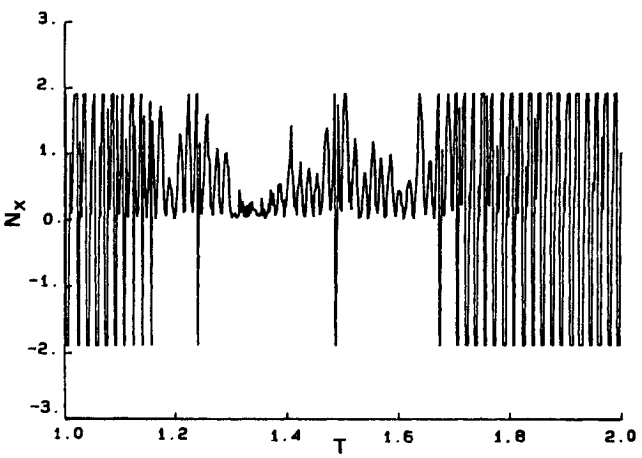

Fig. 7 Time history of dry friction in-plane force for $N_g=12$ kg.

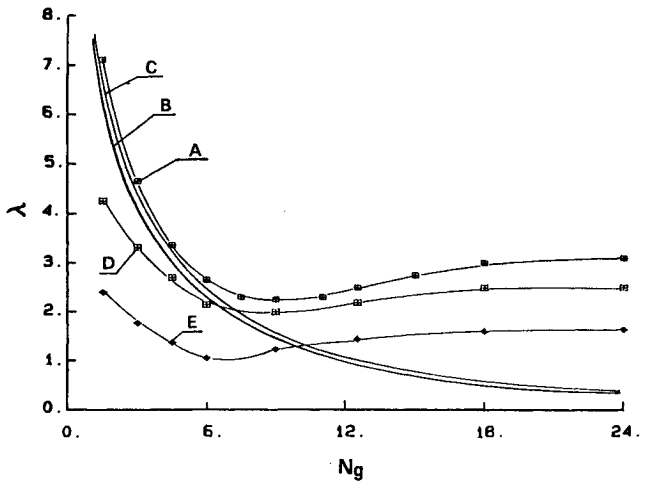

Fig. 6 Mean square response/force λ vs normal load for beam model: A) numerical integration for $\zeta_{e1}=0$, B) approximate solution [Eq. (5)], C) approximate solution [Eq. (6)], D) numerical integration for $\zeta_{e1}=0.006$, E) experiment.

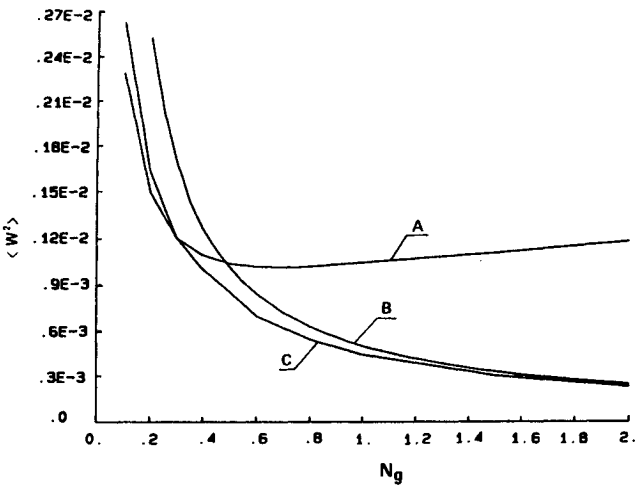

Fig. 8 Mean square response vs normal load for the plate model: A) numerical integration, B) simple approximate solution, C) more accurate approximate solution.

An eight-channel tape recorder (HP 3968A) is used to record all signals. The signal analysis is completed by a multichannel signal processor (Zonic 6088).

The coefficient of dry friction used in the response calculation was determined from the measured value in Ref. 2.

Figure 4 shows the measured PSD from the force transducer under white noise signal source excitation. Although the PSD of the signal source is very flat, the actual force driving the beam is quite different from that of the signal source. The reason is that the dynamic system of the shaker participates in the beam vibration and there is no feedback control system to reject such participation in the random vibration test. Figure 5 shows the measured response PSD and autocorrelation function for normal load $N_g = 6$ kg. The average mean square values of the beam response displacement and input force were measured directly from the autocorrelation function at $t = 0$ or from the integration of the PSD. In this paper, the autocorrelation method is applied to determine the average mean square values. As a check, we also used an integration method of the PSD. The results were in close agreement. The experimental results will be discussed in the following section.

Results and Discussion

In the present calculation the white noise source is from a standard IMSL routine, GGNML, which generates a set of Gaussian random numbers. The PSD of this process is not an ideal white noise. In order to overcome this disadvantage, we use ensemble averaging. Figure 4 shows the input force PSD after 100 ensemble averagings. It basically approaches an ideal white noise, which is a principal basis for the numerical calculation.

Broadband Random Excitation

Figure 6 shows the results of mean square response/force λ vs normal load for the beam model. Curve A is from numerical integration, curve B from the approximate solution of Eq. (5) and curve C from Eq. (6). These curves do not include the beam material damping. Curve D is from a numerical integration with $\zeta_{el} = 0.006$ and Curve E from experiment. It is found that curves B and C are in good agreement because of the well-separated modes; also, in the case of smaller normal load (smaller equivalent damping), the approximate solution coincides with the result from the numerical integration. As the normal load increases, the difference between curves A and B increases. The reason is that slip-stick and stick phenomena occur when the normal load increases. In this case, the energy dissipation due to dry friction at the support boundary tends to vanish and the response amplitude becomes larger. This is also explained by Fig. 7, which shows the calculated time history of the dry friction in-plane force N_x at a normal load of 12 kg. In this figure stick-slip and stick can be observed. Curves D and E in Fig. 6 are used to compare the results from theoretical analysis and experiment. It is found that the agreement is qualitatively good, but not quantitatively good. The measured values are generally lower than theoretical values. The difference comes mainly form the difference in input random force, as shown in Fig. 4. The assumption of the white noise excitation used in calculation does not closely approximate that in the present experimental system.

Figure 8 shows the results of mean square response vs normal loads for the pinned plate. Curve A is from numerical integration; curve B from the simple, approximate solution of Eq. (17), and curve C from the more accurate approximate solution of Eq. (15). The results are similar to those of the beam. There is a much greater difference in curves B and C when the normal load is small. The reason is that curve B does not include the stiffness nonlinearity. For a system with little damping, the mean square response is dominated by the nonlinear stiffness terms. As the damping increases, the effect of the nonlinear stiffness decreases. Curves A and C are very close in the region of small normal load. In the region of middle-to-large normal load, curves A and C are very different. This phenomenon is similar to curves A and C in Fig. 6. In addition, the slip at both edges does not occur simultaneously because of the nonsymmetric driving point.

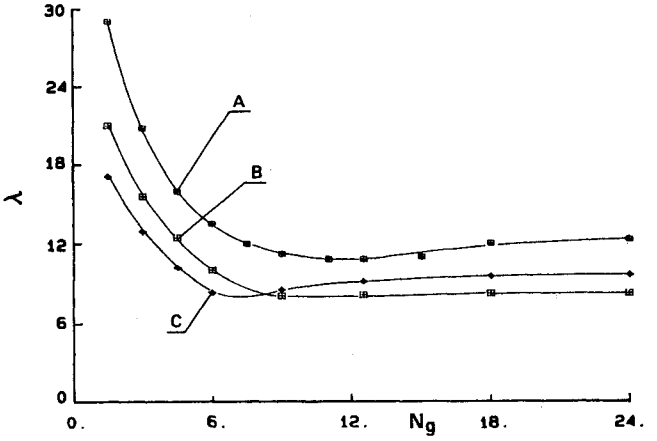

Fig. 10 Mean square response/force λ vs normal load for $f_0 = 28.5$ Hz and $df = 10$ Hz: A) numerical integration for $\zeta_{el} = 0$, B) for $\zeta_{el} = 0.006$, C) experiment.

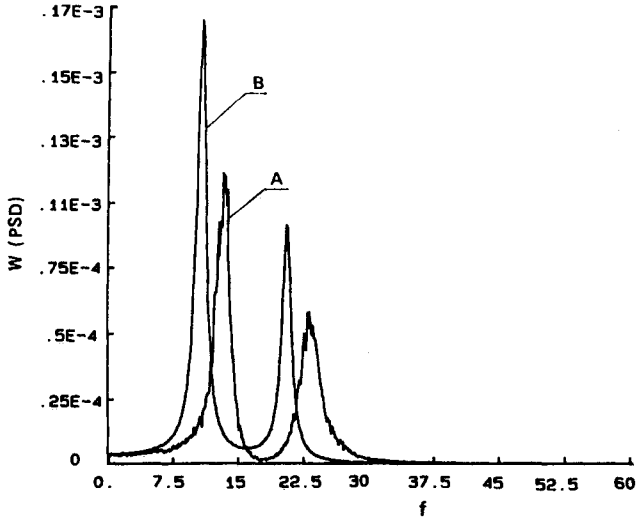

Fig. 9 Response PSD of the plate model for $N_g = 0.1$ kg/cm: A) numerical integration, B) simple approximate solution.

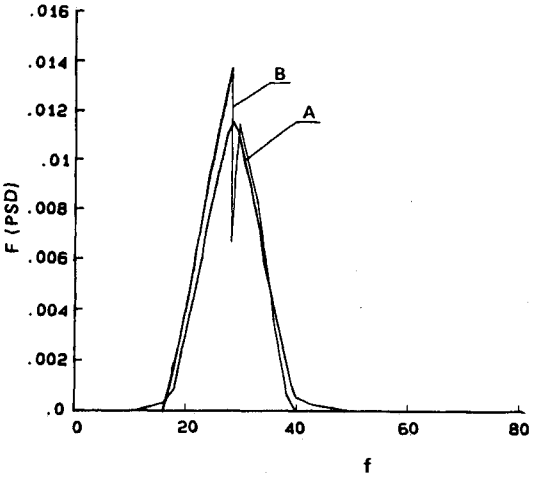

Fig. 11 Input force PSD for $f_0 = 28.5$ Hz and $df = 10$ Hz: A) calculation; B) experiment.

Figure 9 shows the PSD response at normal load 0.1 kg/cm for the pinned plate. Curve A is from numerical integration and curve B from the simple approximate solution. It is found that the peak frequencies (13.25 and 22.8 Hz) for curve A are not equal to the natural frequencies (10.67 and 20.52 Hz) of the plate. The frequency shift comes from the nonlinear stiffness term.

Narrow-Band Random Excitation

Figure 10 shows the results of mean square response/force λ vs normal load for the beam model in the case of center frequency $f_0 = 28.5$ Hz and bandwidth $df = 10$ Hz. Curves A and B are from the numerical integration for $\zeta_{el} = 0$ and $\zeta_{el} = 0.006$, respectively. Curve C is from the experiment. The shape of these curves is very similar to the result from the broadband random excitation. The agreement between theory and experiment is better than that for the broadband excitation. This can be explained by Fig. 11, which shows the PSD of the input random force used in the calculation and also that from the measurement where both have the same mean square input force. The two PSD are in generally close agreement. The principal difference in the two PSDs is that, at the first natural frequency, the measured PSD has a sharp minimum. Compare Figs. 4 and 11 and then Figs. 6 and 10.

Figure 12 shows the experimental results of mean square response/force λ vs normal load for various bandwidth with $f_0 = 28.5$ Hz. It is found that λ increases as df decreases for the same normal load. When the bandwidth becomes narrow, the excitation energy is concentrated in the region near the first natural frequency. The response is dominated by the first mode. All the minima of these curves are located at approximately $N_g = 6$ kg. This normal load may be an optimal value for obtaining maximum damping from slipping at the beam support boundary.

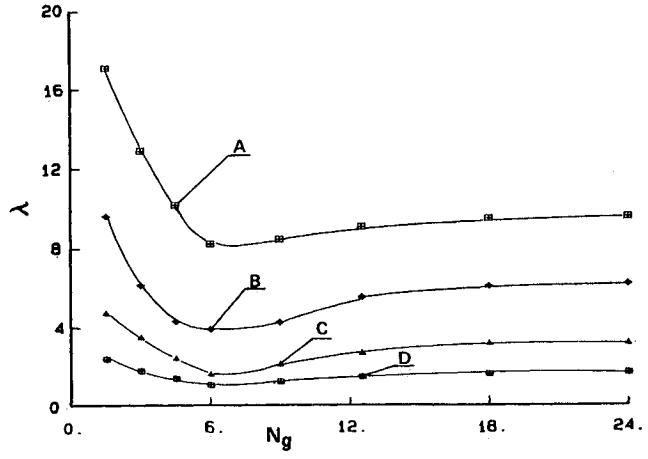

Fig. 12 Experimental mean square response/force λ vs normal loads for various bandwidths: A) $df = 10$ Hz, B) $df = 30$ Hz, C) $df = 100$ Hz, D) white noise.

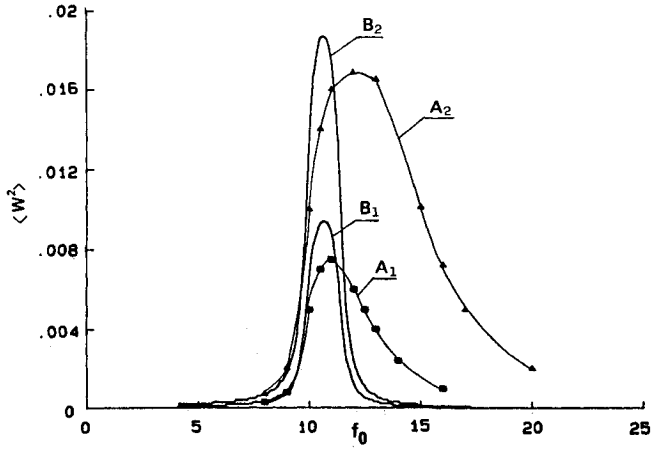

Fig. 13 Mean square response/force λ vs center frequency f_0 at $df = 10$ Hz for the plate model.

Figure 13 shows the result of the mean square response vs center frequency for the pinned plate model at a normal load of 0.1 kg/cm. The first mode ($n_x = 1$, $n_y = 1$) is considered in the figure. Curves A_1 and A_2 are from the numerical integration and curves B_1 and B_2 from the simple approximate solution of Ref. 9. Two different excitation levels are considered. The excitation levels and bandwidth (1.5 Hz) are held nearly constant as the center frequency shifts. Curves A_1 and B_1 are for the lower excitation force $\langle F^2 \rangle = 0.0015$ kg and curves A_2 and B_2 for higher excitation force $\langle F^2 \rangle = 0.003$ kg. From curves B_1 and B_2, the approximate solution predicts no change in damping with the excitation level. However, there is an apparent change in damping seen in the numerical simulation results. This is explained below.

Comparing curves A_1 and B_1, it is found that the peak frequency of curve A_1 corresponds to the first natural frequency of the plate. The peak frequency might have been expected to be higher than the first natural frequency because of the nonlinear stiffness, as shown in Fig. 9. That it is not can be understood as follows. As is well known for sinusoidal excitation from Ref. 2, in the frequency region of 10.67-13.25 Hz, there are three possible response amplitudes, one of which is unstable. For random excitation, the mean square response in this frequency region, therefore, reflects an average response characteristic between the two stable amplitudes found in the sinusoidal excitation case. Hence, the response peak is broader than one might first expect, ranging over a frequency interval determined by the hysterisis induced by the plate nonlinear stiffness. Thus, what might appear to be an increase in damping is really a result of the nonlinear stiffness creating a frequency response hysterisis that, when the plate is randomly excited, leads to a broader peak response. Comparing curves A_1 and A_2, we also find that the response peak becomes broader as the excitation level increases. This is because the nonlinear stiffness effect becomes stronger. For a very low excitation level, it is expected that curves A and B will coincide.

This apparent increase in damping (which is seen to be really a consequence of the nonlinear stiffness effect) has been observed in experimental data by several authors.[10-12] The theoretical explanation offered here is thought to be the first published in the literature.

Conclusions

A numerical and experimental study has been perfomed for the response of a beam and plate with slipping at the support boundaries to random excitation. The following conclusions have been reached:

1) The numerical simulation and experimental results have shown that the equivalent linear viscous damping concept due to slipping at the support boundaries can often be applied to determine with reasonable accuracy the response to random excitation. This procedure greatly simplifes the nonlinear random vibration problem.

2) The comparison between theoretical and experimenal results for narrow bandwidth excitation is better than that for (wide-band) white noise excitation. However, this is thought to be principally a consequence of the wide-band excitation in the experiment deviating substantially from the ideal white noise excitation assumed in the calculation.

3) The response of the plate due to narrow-band excitation appears to show an increase in damping as the excitation level increases. In fact, the result is really a consequence of the nonlinear stiffness effect.

Acknowledgment

This work was supported by the U.S. Air Force Office of Scientific Research, Grant 83-0346. Dr. Anthomy Amos is the technical monitor.

References

[1]Dowell, E. H., "Damping in Beams and Plates Due to Slipping at the Support Boundaries, Part 1: Theory," *Journal of Sound and Vibration*, Vol. 105, No. 2, 1986, pp. 243-253.

[2]Tang, D. M. and Dowell, E. H., "Damping in Beams and Plate Due to Slipping at the Support Boundaries, Part 2: Numerical and Experimental Study," *Journal of Sound and Vibration*, (to be published).

[3]Booton, R. C., "The Analysis of Nonlinear Control Systems with Random Inputs," *IRE Transactions on Circuit Theory*, Vol. 1, 1954, pp. 32-34.

[4]Caughey, T. K., "Equivalent Linearization Technique," *Journal of the Acoustical Society of America*, Vol. 35, No. 11, 1963, pp. 1706-1711.

[5]Atalik, T. S., "Stochastic Linearization of Multi-Degree-of-Freedom Nonlinear Systems," *Earthquake Egnineering and Structural Dynamics*, Vol. 4, 1976, pp. 411-420.

[6]Fang, T. and Wang, Z., "A Generalization of Caughey's Normal Mode Approach to Nonlinear Random Vibration Problems," *AIAA Journal*, Vol. 24, No. 3, 1986, pp. 531-534.

[7]Lin, Y. K., *Probabilistic Theory of Structural Dynamics*, McGraw-Hill Book Co., New York, 1967.

[8]Fralich, R. W., "Postbuckling Effects on the Flutter of Simply Supported Rectangular Panels at Supersonic Speeds," NASA TN D-1615, 1963.

[9]Crandall, S. H. and Mark, W. D., *Random Vibration in Mechanical Systems*, Academic Press, New York and London, 1963.

[10]White, R. G., "Comparison of the Statistical Properties of the Response of Aluminum Alloy and CRFP Plates to an Acoustic Excitation," *Composites*, Vol. 9, No. 4, 1978, pp. 251-258.

[11]Wentz, K. R., and Mei, C., "Experimental Nonlinear Response of Panels Subjected to High Intensity Noise," AIAA Paper 81-0631, 1981.

[12]Soovere, J., "Sonic Fatigue Testing of an Advanced Composite Aileron," *Journal of Aircraft*, Vol. 19, No. 4, 1982, pp. 304-310.